J. Phase Equilib. Diffus. (2018) 39:57–67
https://doi.org/10.1007/s11669-017-0607-y

Thermodynamic Description of Al-Si-Mg-Ce Quaternary System in Al-Rich Corner and Its Experimental Validation

Zhao Lu[1] · Xi Li[2,3] · Lijun Zhang[1]

Submitted: 6 July 2017 / in revised form: 17 September 2017 / Published online: 15 November 2017

Abstract In order to establish a self-consistent thermodynamic database for Al-Si-Mg-Ce quaternary system, all the thermodynamic descriptions of 6 boundary binaries, i.e., Al-Mg, Al-Si, Al-Ce, Mg-Si, Mg-Ce, and Si-Ce were first unified. Then, the thermodynamic descriptions for ternary Al-Mg-Ce system were re-assessed using the CALculation of PHAse Diagrams (CALPHAD) method based on all the critically reviewed experimental phase equilibria. Moreover, the consistency between thermodynamic descriptions for Al-Si-Ce ternary system and those for the unified binaries was checked and confirmed. Subsequently, the thermodynamic database for the Al-Si-Mg-Ce quaternary system was established by combining the four ternary subsystems, and the phase equilibria/thermodynamic properties of the quaternary system were predicted via direct extrapolation from the ternary systems. The reliability of the established database was finally validated in one Al-7Si-0.6Mg-0.4Ce quaternary model alloy by comprehensively comparing its experimentally measured phase transition temperatures and solidified microstructure characteristics with the Gulliver-Scheil simulation ones. Good agreement between the thermodynamic predictions and experimental results indicates the present thermodynamic database is reliable.

✉ Lijun Zhang
xueyun168@gmail.com; lijun.zhang@csu.edu.cn

[1] State Key Lab of Powder Metallurgy, Central South University, Changsha 410083, China

[2] School of Mechanical, Material, Mechatronic and Biomedical Engineering, University of Wollongong, Wollongong, NSW 2522, Australia

[3] Australian Nuclear Science and Technology Organisation, Lucas Heights, NSW 2234, Australia

Keywords Al-Si-Mg-Ce system · CALPHAD · Gulliver-Scheil simulation · phase diagram

1 Introduction

Aluminium-silicon casting alloys are widely used i.e., in the automobile industry where involves a specific feature like high strength-to-weight ratio and low fuel consumption due to their low density, high corrosion resistance, good wear resistance and castability.[1] Addition of magnesium can improve the heat-treatment responsiveness and thus increase the corrosion resistance and tensile properties of the alloys.[2,3] In the traditional Al-Si-Mg castings, the presence of coarse primary aluminium and plate-like eutectic silicon, which results in poor mechanical properties, is undesirable. Therefore, the grain refinement is usually required in Al-Si-Mg castings to obtain the equiaxed primary aluminium and fibrous eutectic silicon particle for improving their performance.[4]

Rare earth metals, such as cerium (Ce), have been found to improve the mechanical properties and ductility of Al-Si-Mg alloys through modifying their microstructure.[5] It was reported that the Al-Si-Mg alloys with cerium addition exhibit better microstructure due to the formation of intermetallic phases with Ce, which may act as nucleation sites for primary aluminium or suppress the growth rate of silicon crystals.[6] For a better understanding of the nature of the solidified phases and their relative amounts as well as solidification sequence, the accurate phase diagram and thermodynamic properties of the quaternary Al-Si-Mg-Ce system in Al-rich corner are necessary.

The CALculation of PHAse Diagrams (CALPHAD) approach has become a valuable tool to calculate phase equilibrium and solidification sequences of the multi-

component system. The key to perform accurate CALPHAD-type thermodynamic calculations lies in the reliability of the established thermodynamic descriptions for the target alloy. Although the thermodynamic descriptions for the boundary ternaries in quaternary Al-Si-Mg-Ce system have been reported,[7–10] a simple extrapolation of the reported ternary systems into the quaternary Al-Si-Mg-Ce system is impossible, due to the inconsistent thermodynamic descriptions of the boundary binaries utilized in those ternary systems. Therefore, there is a need to unify the thermodynamic descriptions for the boundary binary systems in the Al-Si-Mg-Ce quaternary system and re-assess the boundary ternaries if necessary, from which a self-consistent thermodynamic database for the Al-Si-Mg-Se system can then be established.

Consequently, the major objectives of the present study are: (1) to unify the thermodynamic descriptions of the boundary binaries in Al-Si-Mg-Ce quaternary system and re-assess the thermodynamic descriptions for the Al-Mg-Ce system based on the updated binaries by means of the CALPHAD method; (2) to establish a self-consistent thermodynamic description of the Al-Si-Mg-Ce quaternary system based on direct extrapolation from the boundary ternaries; (3) to verify the reliability of the established thermodynamic descriptions in Al-rich corner by comparing the model-predicted microstructure information in one key quaternary alloy using the Gulliver-Scheil simulation with the experimental microstructure after solidification.

2 Literature Review

2.1 Binary Systems

There are six boundary binaries in the Al-Si-Mg-Ce system. The thermodynamic descriptions for Al-Si,[7] Al-Mg,[7] Si-Mg[7] were already critically assessed in our research group, and are directly utilized here. For the Al-Ce system, there are several reported sets of thermodynamic descriptions.[11–13] To ensure the compatibility of the models and thermodynamic parameters of binary Al-Ce with higher-order systems, we cannot directly use the very recently thermodynamic descriptions for the Al-Ce system given by Jin et al.[13] since they adopted modified quasi-chemical model for liquid phase. Based on the critically experimental measurements, Gao et al.[12] found that Al_2Ce should be treated as linear compound rather than Laves phase (C15, prototype Cu_2Mg),[11] and that there is an $\alpha/\beta Al_3Ce$ polymorphous transition at 973 °C. Moreover, such observation of Gao et al.[12] was further confirmed by Jin et al.[13] Thus the set of thermodynamic parameters reported by Gao et al.[12] was accepted in the present work. For the Si-Ce system, its thermodynamic description was obtained from the published report by Ref 8. As for the binary Mg-Ce system, two sets of thermodynamic descriptions were given by Cacciamani et al.[14] and Zhang et al.[15] respectively. They exhibit large discrepancies in both Ce- and Mg-rich sides. It is found that the solubility range of bcc phase assessed by Zhang et al.[15] is more consistent with experimental data. However, the enthalpies of formation of $Mg_{17}Ce_2$, $Mg_{41}Ce_5$ and $Mg_{12}Ce$ intermetallics are too negative given by Zhang et al.[15] and thus cause Mg-Ce system difficulty in achieving compatibility with higher-order systems. Li et al.[16] updated the thermodynamic description for the Mg-Ce system based on the work of Zhang et al.[15] and it was thus directly adopted here.

2.2 Ternary Systems

In the aspect of boundary ternaries, because the binary systems Al-Si, Al-Mg, and Si-Mg adopted in this work are the same as those used in the ternary Al-Si-Mg system by Tang et al.[7] we directly applied their ternary interaction parameters[7] in the current Al-Si-Mg system. For the ternary Al-Si-Ce, the first isothermal section in Ce-poor region at 400 °C was given by Altunina et al.[17] They reported the existence of one ternary compound with the composition $Ce_{20}Al_{35}Si_{45}$ (at.%) and a composition range for mixed crystals $CeAl_xSi_{2-x}$ ($\alpha ThSi_2$) with Al range up to $x = 1.8$. Raman et al.[18] prepared the Al-Ce-Si alloys by arc melting. The samples were then wrapped in molybdenum foil, which was followed by heating in evacuated silica capsules at 1000 °C for 96 h and slow cooling in air. They found a different phase $CeAl_{1.625}Si_{0.375}$ with AlB_2 structure type, which contradicts the wide composition range of $CeAl_xSi_{2-x}$ observed by Altunina et al.[17] The existence of $CeAl_{1.625}Si_{0.375}$ phase was further confirmed by Muraveva[19] at 500 °C in an investigation of the isothermal section of Al-Ce-Si system. Two additional ternary phases $AlCeSi_2$ and $Al_4Ce_3Si_6$ at 500 °C were given by Flandorfer et al.[20,21] The crystal structures of this two compounds were analyzed on the annealed samples by Paterson and Fourier methods and full-matrix Rietveld refinement. Recently, Grobner et al.[8] presented a systematic investigation of Al-Si-Ce. They found that though a ternary compound $Al_4Ce_3Si_6$ appears after annealing an arc-melted Al_2CeSi_2 at 500 °C for 336 h, it disappears when the annealing time prolongs to 870 h. Therefore, it is reasonable to regard Al_2CeSi_2 and $Al_4Ce_3Si_6$ compounds to be not stable phase. The microstructures of the samples $Al_{90}Ce_{8.0}Si_{2.0}$, $Al_{90}Ce_{7.0}Si_{3.0}$, $Al_{90}Ce_{5.7}Si_{4.3}$, and $Al_{90}Ce_{2.6}Si_{7.4}$ showed that $Al_{11}Ce_3$ was primary crystallized phase only in the Si-poor sample $Al_{90}Ce_{8.0}Si_{2.0}$, while the phase τ_1-$Ce(Si_{1-x}Al_x)_2$ solidified as the primary phase in other samples.[8]

Moreover, they also confirmed a transition reaction $L + \tau_1 \rightarrow \tau_2$-$AlCeSi_2$ +(Al) at 621 °C using the DSC measurement. By coupling reliable experimental data in literature with their own experimental results, a thermodynamic assessment of Al-Ce-Si system was further performed by Gröbner et al.[8] The ternary interaction parameters evaluated by Gröbner et al.[8] together with the updated boundary binaries described here can exactly reproduce all the experimental phase equilibria utilized in the assessment of Ref 8. Thus, the ternary interaction parameters in the Al-Si-Ce system from Gröbner et al.[8] were directly accepted here.

The partial isothermal section of the Al-Mg-Ce system with Ce composition up to 33.3 at.% at 400 °C was first studied by Zarechnyuk et al.[22] They reported a ternary compound $Al_{67}Ce_5Mg_{28}$ with the Laves $MgZn_2$ structure type. Based on 6 arc-melted samples annealed at 400 °C for 608 h, Cui et al.[23] reported two ternary compounds, i.e., Al_4CeMg_4 and $Al_{21}CeMg_8$, by means of metallographic analysis. However, the crystal structures of the two compounds were not determined by Ref 23 and their existence was not confirmed in the later studies.[9,10,24,25] Zheng et al.[18] determined a small portion of the Al-rich liquidus surface and a eutectic reaction, L = (Al) + $Al_{11}Ce_3$ + β ($Al_{140}Mg_{89}$), occurring at 446 °C by using thermal analysis (TA). A more detail investigation of the Al-Mg-Ce system was conducted by Odineav,[24,25] who reported a new ternary compound $Al_2Ce_{0.8}Mg_{0.2}$ with the congruent melting point of 635 °C. Based on x-ray powder diffraction (XRD) analysis, they claimed that this compound is the same as that reported by Zarechnyuk et al.[22] and both belong to the Laves $MgZn_2$ structure type. Besides, Odineav et al.[24] also determined the solubility of Al in $CeMg_2$, CeMg and $CeMg_{12}$ at 400 °C and 7 invariant reactions[25] by means of XRD and differential themal analyzer (DTA), respectively. Gröbner et al.[9] employed several key alloys to measure the isothermal section of the Al-Mg-Ce system at 400 °C. All the samples were sealed in evacuated silica tubes and annealed at 400 °C for 500 h. They suggested that the ternary compound $Al_{13}CeMg_6$ melted incongruently at T = 455 °C. Based on the XRD results, three other ternary compounds, including Ce(Mg,Al), $Ce(Mg,Al)_2$ and $Ce(Mg,Al)_{12}$, were also observed in the Al-Mg-Ce system.[9] Based on the literature data and their own experiments, Gröbner et al.[9] performed a thermodynamic assessment of the ternary Al-Mg-Ce system using the Calphad method. After that, Jin et al.[10] prepared $Mg_{0.6667}Ce_{0.3333}$ and $Al_{0.6667}Ce_{0.3333}$ samples by arc melting under purified argon, assembled the samples into one solid-liquid diffusion couple and annealed it at 400 °C for 4 weeks. Based on the electron probe microanalyzer (EPMA) and XRD analysis, the ternary phases $Al_{13}CeMg_6$, BCC_B2 and Laves_C15 were reported. Very recently, two of the present authors, Lu and Zhang,[26] investigated the thermal stability of $Al_{13}CeMg_6$ compound by integrating DSC, XRD and EPMA techniques. They determined that the crystal structure of $Al_{13}CeMg_6$ compound is $MgNi_2$ structure using the Rietveld method. Moreover, they also observed that the $Al_{13}CeMg_6$ melts at 492.1 °C via a peritectic reaction: liquid + $Al_{11}Ce_3 \rightarrow Al_{13}CeMg_6$ and decomposes at a certain temperature between 320 and 400 °C with a eutectoid reaction: $Al_{13}CeMg_6 \rightarrow Al_{11}Ce_3 + Al_3Mg_2$. However, the experimental phase equilibria by Ref 9, 24–26 cannot be well described by the reported ternary interaction parameters[9,10] in combination with the updated boundary binaries. Hence, there is a significant necessary to re-assess the thermodynamic descriptions for the Al-Mg-Ce system to reproduce the experimental data in literature. In the present thermodynamic assessment, the experimental data from Odineav et al.[24] Gröbner et al.[9] and Lu and Zhang[26] were taken in account, while the experimental data on liquid surface of the Al-Mg-Ce system from Ref 25, 27 were not considered due to the large uncertainty of the data.

For the Mg-Si-Ce boundary ternary, its thermodynamic descriptions can be directly extrapolated from the corresponding binary boundaries because no ternary phase has been reported in the Mg-Si-Ce system and we only focus on the Al-rich phase equilibria of the Al-Si-Mg-Ce quaternary system. For the Al-Si-Mg-Ce quaternary system, no any reports on the experimental phase equilibria/thermochemical data are available in the literature, and thus a direct extrapolation of the boundary ternaries was made for Al-Si-Mg-Ce system.

3 Thermodynamic Models

According to the critically reviewed information above, Ce(Mg,Al), $Ce(Mg,Al)_2$, $Ce(Mg,Al)_{12}$ and $Al_{13}CeMg_6$ phases were considered in the Al-Mg-Ce ternary system. For the quaternary system, liquid, fcc_A1 (Al, αCe), bcc_A2 (βCe), hcp_A3 (Mg), and diamond (Si) solution phases were included. Considering no any experimental information on the solubility of fourth element in ternary compounds, all the ternary compounds are treated as pure ternary ones in quaternary Al-Si-Mg-Ce system. The thermodynamic models for all the involved phases are presented concisely as follows.

3.1 Liquid and Solid Solution Phases

The liquid, fcc_A1 (Al, αCe), bcc-_A2 (βCe), hcp-_A3 (Mg), and diamond (Si) phases are described by the substitutional solution model. Taking the liquid phase for example, its molar Gibbs energy is expressed by the following equations[28,29]

$$G^{\text{liquid}} = {}^{\text{ref}}G^{\text{liquid}} + {}^{\text{mix}}G^{\text{liquid}} + {}^{\text{ex}}G^{\text{liquid}}_{\text{bin}} + {}^{\text{ex}}G^{\text{liquid}}_{\text{ter}} \quad \text{(Eq 1)}$$

with

$${}^{\text{ref}}G^{\text{liquid}} = x_{\text{Al}}{}^{0}G^{\text{liquid}}_{\text{Al}} + x_{\text{Si}}{}^{0}G^{\text{liquid}}_{\text{Si}} + x_{\text{Mg}}{}^{0}G^{\text{liquid}}_{\text{Mg}} + x_{\text{Ce}}{}^{0}G^{\text{liquid}}_{\text{Ce}} \quad \text{(Eq 2)}$$

$${}^{\text{mix}}G^{\text{liquid}} = \text{R}T \cdot \left(x_{\text{Al}} \ln x_{\text{Al}} + x_{\text{Si}} \ln x_{\text{si}} + x_{\text{Mg}} \ln x_{\text{Mg}} + x_{\text{Ce}} \ln x_{\text{Ce}}\right) \quad \text{(Eq 3)}$$

$$\begin{aligned}
{}^{\text{ex}}G^{\text{liquid}}_{\text{bin}} = {} & x_{\text{Al}}x_{\text{Si}} \sum_{i=0}^{n} (x_{\text{Al}} - x_{\text{Si}})^{i} \cdot L^{i}_{\text{AlSi}} \\
& + x_{\text{Al}}x_{\text{Mg}} \sum_{i=0}^{n} (x_{\text{Al}} - x_{\text{Mg}})^{i} \cdot L^{i}_{\text{AlMg}} \\
& + x_{\text{Al}}x_{\text{Ce}} \sum_{i=0}^{n} (x_{\text{Al}} - x_{\text{Ce}})^{i} \cdot L^{i}_{\text{AlCe}} \\
& + x_{\text{Si}}x_{\text{Mg}} \sum_{i=0}^{\text{n}} (x_{\text{Mg}} - x_{\text{Si}})^{\text{i}} \cdot L^{i}_{\text{SiMg}} \\
& + x_{\text{Si}}x_{\text{Ce}} \sum_{i=0}^{n} (x_{\text{Ce}} - x_{\text{Si}})^{i} \cdot L^{i}_{\text{SiCe}} \\
& + x_{\text{Mg}}x_{\text{Ce}} \sum_{i=0}^{n} (x_{\text{Ce}} - x_{\text{Mg}})^{i} \cdot L^{i}_{\text{MgCe}}
\end{aligned} \quad \text{(Eq 4)}$$

$$\begin{aligned}
{}^{\text{ex}}G^{\text{liquid}}_{\text{ter}} = {} & x_{\text{Al}}x_{\text{Si}}x_{\text{Mg}} \sum_{i=\text{Al,Si,Mg}}^{n} [x_i + (1 - x_{\text{Al}} - x_{\text{Si}} - x_{\text{Mg}})/3] \cdot L^{i}_{\text{AlSiMg}} \\
& + x_{\text{Al}}x_{\text{Si}}x_{\text{Ce}} \sum_{i=\text{Al,Si,Ce}}^{n} [x_i + (1 - x_{\text{Al}} - x_{\text{Si}} - x_{\text{Ce}})/3] \cdot L^{i}_{\text{AlSiCe}} \\
& + x_{\text{Al}}x_{\text{Mg}}x_{\text{Ce}} \sum_{i=\text{Al,Mg,Ce}}^{n} [x_i + (1 - x_{\text{Al}} - x_{\text{Mg}} - x_{\text{Ce}})/3] \cdot L^{i}_{\text{AlMgCe}} \\
& + x_{\text{Mg}}x_{\text{Si}}x_{\text{Ce}} \sum_{i=\text{Mg,Si,Ce}}^{n} [x_i + (1 - x_{\text{Mg}} - x_{\text{Si}} - x_{\text{Ce}})/3] \cdot L^{i}_{\text{MgSiCe}}
\end{aligned} \quad \text{(Eq 5)}$$

where x_i (i = Al, Si, Mg or Ce) is the mole fraction of element i, R is the gas constant, and T is the temperature in Kelvin. ${}^{0}G^{\text{liquid}}_{i}$ (i = Al, Si, Mg or Ce) is the molar Gibbs energy of the pure element i in the liquid state, which can be directly taken from the compilation of Dinsdale.[30] L^{i}_{AB} (A, B = Al, Si, Mg or Ce, and A ≠ B), and L^{i}_{ABC} (A, B, C = Al, Si, Mg or Ce, and A ≠ B ≠ C) are the binary, ternary, and interaction parameters, respectively. All of these parameters are temperature-dependent, and usually expressed as $a+b \cdot T$, and thus the interaction parameters are termed as $as+bs \cdot T$. The interaction coefficients, as and bs, are either optimized based on the experimental data or computed from first-principles calculations.[31]

3.2 Intermetallic Compounds

Taking into account the fact that there is a continuous solid solution CeM_2 between the binary $CeAl_2$ and $CeMg_2$ phases and the crystal structures of both $CeAl_2$ and $CeMg_2$ belong to Cu_2Mg,[9,24,25] the CeM_2 phase is described by the sublattice model $Ce_1(Al,Mg)_2$. The other two analogous ternary solid solutions CeM and CeM_{12} are modeled with $Ce_1(Al,Mg)_1$ and $Ce_1(Al,Mg)_{12}$, respectively. According to the formula for the sublattice model,[32] the molar Gibbs energy of the representative CeM_2 is expressed as

$$\begin{aligned}
G^{CeM_2} = {} & y_{\text{Al}}G^{0,\text{CeM}_2}_{\text{Ce:Al}} + y_{\text{Mg}}G^{0,\text{CeM}_2}_{\text{Ce:Mg}} \\
& + 0.66667\text{R}T \cdot \left(y_{\text{Al}} \ln y_{\text{Al}} + y_{\text{Mg}} \ln y_{\text{Mg}}\right) \\
& + y_{\text{Al}}y_{\text{Mg}}L^{0,\text{CeM}_2}_{\text{Ce:Al,Mg}} + y_{\text{Al}}y_{\text{Mg}}\left(y_{\text{Al}} - y_{\text{Mg}}\right)L^{1,\text{CeM}_2}_{\text{Ce:Al,Mg}}
\end{aligned} \quad \text{(Eq 6)}$$

where y_{Al} and y_{Mg} are the site fractions of Al and Mg on the second sublattice. The two end-members $G^{0,\text{CeM}_2}_{\text{Ce:Al}}$ and $G^{0,\text{CeM}_2}_{\text{Ce:Mg}}$, also named as the compound energies, are expressions relative to the Gibbs energy of fcc_A1 Al, hcp_A3 Mg and fcc_A1 Ce at the same temperature. $L^{0,\text{CeM}_2}_{\text{Ce:Al,Mg}}$ and $L^{1,\text{CeM}_2}_{\text{Ce:Al,Mg}}$ are the ternary interaction parameters, which can be optimized from the available experimental data. Analogous expressions can be written for the Gibbs energies of the other two phases CeM and CeM_{12}.

The remaining $Al_{13}CeMg_6$ ternary compound is considered as a stoichiometric compound due to the negligible homogeneity range according to Ref 9,10,26 Thus, the molar Gibbs energy for $Al_{13}CeMg_6$ (τ) is expressed relative to the mechanical mixing of the pure elements via the following equation:

$${}^{0}G^{\tau} - 0.65\,G^{\text{fcc\_A1}}_{\text{Al}} - 0.05\,G^{\text{fcc\_A1}}_{\text{Ce}} - 0.3\,G^{\text{hcp\_A3}}_{\text{Mg}} = e + f \cdot T \quad \text{(Eq 7)}$$

in which the coefficients e and f are to be evaluated in the present work.

4 Experimental Procedure

In order to validate the reliability of the established thermodynamic database for the quaternary Al-rich Al-Si-Mg-Ce system, one key model alloy, i.e., Al-7Si-0.6Mg-0.4Ce (in wt.%), was prepared and its as-cast microstructure information and transition temperatures served as the experimental basis.

High-purity elements of Al (purity: 99.999 wt.%), Si (purity: 99.99 wt.%), Mg (purity: 99.99 wt.%), and Ce (purity: 99.99 wt.%) purchased from Alfa Aesar (China)

Chemicals Co., Ltd. were used to minimize any potential effects from possible contamination by tracer elements. All the compositions hereinafter are expressed as a weight percentage unless otherwise specified. Al-7Si-0.6Mg alloy was first placed in a graphite crucible, and then melted in an induction furnace under an argon gas atmosphere. Since Mg is prone to evaporation during melting, 5% excess of Mg was used. After being homogenized at about 720 °C for 5 min, an Al-2Ce master alloy was then added at a holding temperature of 750 °C to attain the required chemical compositions. Subsequently, the melt was slowly solidified in the graphite crucible by shutting off the furnace power so that each relevant phase is sufficiently grown to allow clear detection. The chemical composition of the sample was measured by inductively coupled plasma (ICP) and further confirmed by chemical analysis (CA). The results show that the maximum deviation from the designed alloy compositions is 0.02 wt.%.

To determine the phase transition temperatures of the model alloy, differential scanning calorimetry (DSC; DSC404C, Netzsch, Germany) measurement was performed on this alloy using a Pt-Pt/Rh thermocouple. The accuracy for temperature measurement was estimated to be ± 1.5 °C.

The sample was subject to microstructural observation. Specimen was taken from the center of as-cast ingot by wire-electrode cutting, then mechanically ground and further polished on automatic polishing equipment using an oxide polishing suspension (OP-S) at a rotation speed of 250 rpm. The micrograph sample was analyzed by the back-scattered electron (BSE) image (JXA-8530, JEOL, Japan), equipped with an electron probe microanalyzer (EPMA; JXA-8530, JEOL, Japan). The volume fractions of relevant phases in the alloy were measured with the linear intercept method[33] using an Image-Pr plus 6.0 metallographic analyzer. At least four different image views were obtained for the specimen.

5 Results and Discussion

5.1 Thermodynamic Descriptions for Ternary Al-Si-Ce and Al-Mg-Ce Systems

The thermodynamic optimization was performed using the PARROT module incorporated in Thermo-Calc software,[34] which minimizes the sum of the squared differences between the experimental and calculated values. The weight for experimental data is chosen based on the reliability of the original literature, and the finally obtained parameters are given in Table 1.

The calculated phase diagrams of Al-Ce, Si-Ce, and Mg-Ce sub-binary systems according to the respective thermodynamic descriptions by Ref 8, 12, 16 adopted in the present work are shown in Fig. 1. The calculated phase diagram of Mg-Ce is compared with the experimental data.[35–38] As can be seen in Fig. 1(c) and (d), there exists a reasonable agreement between the calculated phase equilibria and the experimental ones except for the point at low temperature by Saccone et al.[35] In fact, Saccone et al.[35] observed five thermal signals on $Ce_{94}Mg_4$ (in at.%) sample by using Smith thermal analysis technique, i.e., 789.4 °C (liquidus), 775.4, 606.3, 584.7 and 431.9 °C, but very small thermal effect occurred in solid-state transformation at the lowest temperature.[35] It means that it is difficult to determine the accurate thermal signal using the thermal analysis technique. Thus, in the original work of Li et al.[16] they put lower weight on the last signal (i.e., 431.9 °C) during the assessment of binary Mg-Ce system. That is why the calculated solvus of fcc-(Ce) phase exhibits a certain deviations from the experimental data of Saccone.[35] Figure 2(a) presents the calculated isothermal section of the Al-Si-Ce at 500 °C, while Fig. 2(b) and (c) displays the vertical sections along $Al_{0.9}Ce_{0.1}$-$Al_{0.9}Si_{0.1}$ and $Ce_{0.2}Si_{0.8}$-$Al_{0.8}Ce_{0.2}$ according to the thermodynamic descriptions for boundary binaries[7,8,12] and the ternary

Table 1 Summary of the thermodynamic parameters in the Al-Mg-Ce system

MCe: model $(Al,Mg)_{0.5}Ce_{0.5}$

$${}^0G^{MCe}_{Al:Ce} - 0.5\cdot {}^0G^{fcc\_A1}_{Al} - 0.5\cdot {}^0G^{fcc\_A1}_{Ce} = 2500$$

$${}^0L^{MCe}_{Al,Mg:Ce} = -80000 + 50\cdot T$$

M_2Ce: model $(Al,Mg)_{0.6667}Ce_{0.3333}$

$${}^0L^{MCe}_{Al,Mg:Ce} = -16667 + 3.333\cdot T$$

$${}^1L^{MCe}_{Al,Mg:Ce} = 16667$$

$M_{12}Ce$: model $(Al,Mg)_{0.9231}Ce_{0.0769}$

$${}^0G^{M_{12}Ce}_{Al:Ce} - 0.9231\cdot G^{fcc\_A1}_{Al} - 0.0769 G^{fcc\_A1}_{Ce} = -76923$$

$${}^0L^{M_{12}Ce}_{Al,Mg:Ce} = 6154$$

$Al_{13}CeMg_6$: model $Al_{0.65}Ce_{0.05}Mg_{0.3}$

$${}^0G^{Al_{13}CeMg_6}_{Al:Ce:Mg} - 0.65\cdot G^{fcc\_A1}_{Al} - 0.05\cdot G^{fcc\_A1}_{Ce} - 0.3\cdot G^{hcp\_A3}_{Mg} = -11625 + 0.5\cdot T$$

Unit in J/mole-atom for Gibbs energy, Kelvin for T

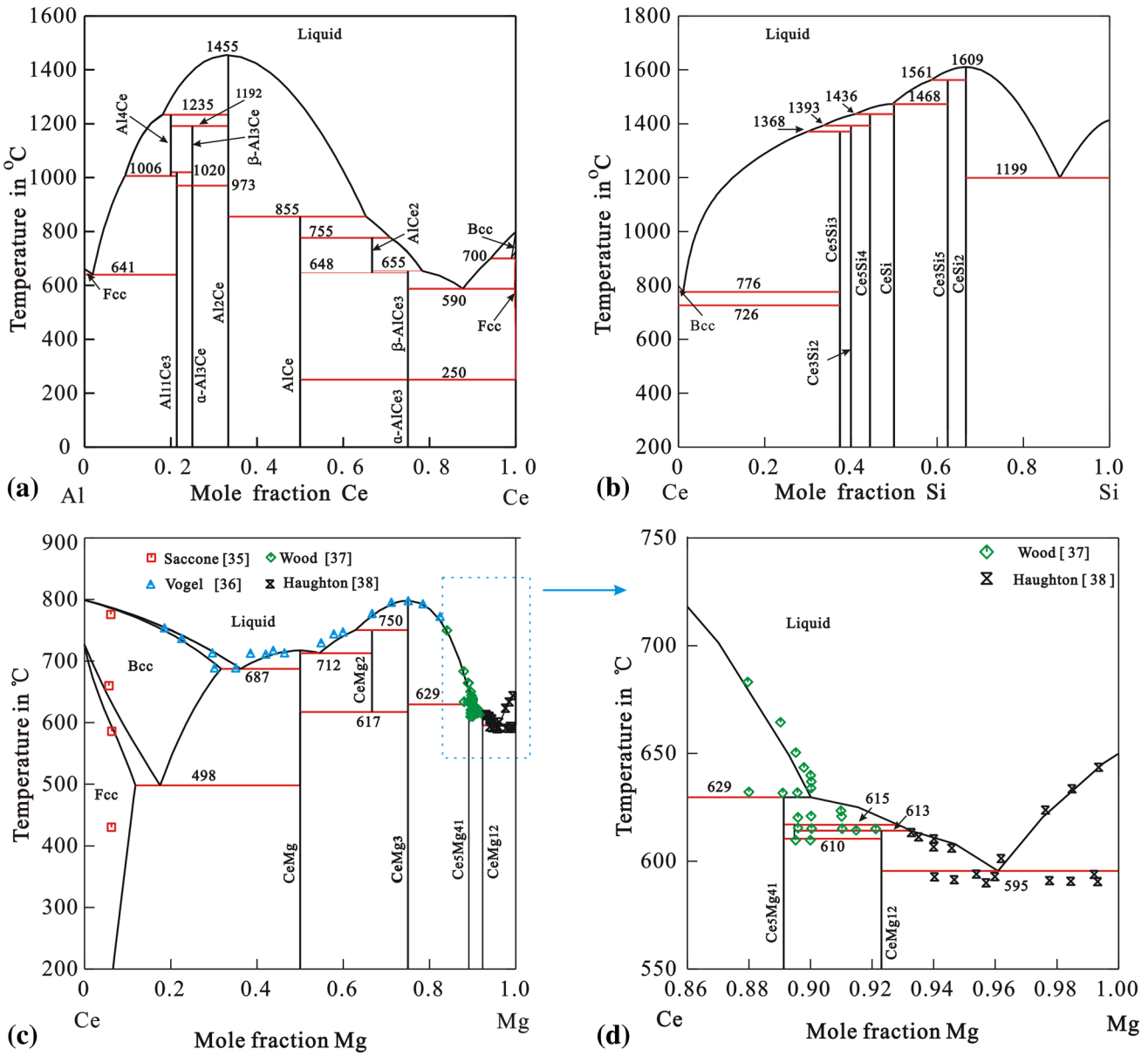

Fig. 1 Calculated phase diagrams of, (a) Al-Ce, (b) Si-Ce binary systems according to the thermodynamic descriptions reported by Gao et al.[12] and Gröbner et al.[8] respectively. Calculated (c) phase diagram of Mg-Ce and (d) its enlarged part in Mg-rich corner according to the thermodynamic descriptions reported by Li[16] compared with the experimental data[36–38]

interaction parameters by Ref 8. The corresponding experimental data from Grönber et al.[8] and Flandorfer et al.[21] are also superimposed for a direct comparison. As can be seen, the calculated results exhibit the excellent consistency with all the experimental data.[8,21] This fact indicates that the unified binary descriptions for the binaries Al-Si,[7] Al-Ce[12] and Si-Ce[8] are consistent with the ternary interaction parameters from Gröbner et al.[8]

The calculated isothermal section of the Al-Mg-Ce system at 400 °C according to the presently evaluated thermodynamic descriptions compared with the experimental data[9,24] is shown in Fig. 3(a). As can be seen in the figure, most of the experimental data can be well reproduced by the present calculations. It can also be indicated that CeAl and CeMg are partially miscible because they have different crystal structures. Though the $CeMg_2$ is metastable in binary Ce-Mg system at 400 °C, it is stabilized by Al in the ternary system. The $CeMg_2$ and $CeAl_2$ form a solid solution with a miscibility gap at 400 °C since they have the same structure. This is in good agreement with the previous assessment by Gröbner et al.[9] Figure 3(b) shows the calculated vertical section

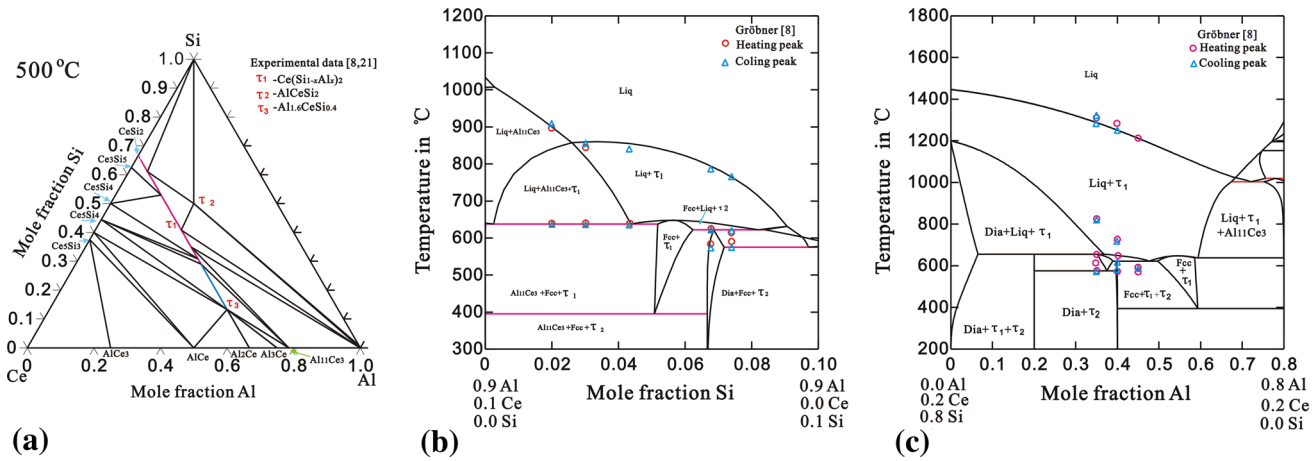

Fig. 2 (a) Calculated isothermal section of the Al-Ce-Si ternary system at 500 °C according to the thermodynamic descriptions for boundary binaries[7,8,12] and the ternary interaction parameters by Ref 8. Calculated vertical sections along (b) Al0.9Ce0.1-Al0.9Si0.1 (in mole fraction) and (c) Ce0.2Si0.8-Al0.8Ce0.2 (in mole fraction) according to the thermodynamic descriptions for boundary binaries[7,8,12] and the ternary interaction parameters by Ref 8 compared with the corresponding experimental data[8,21]

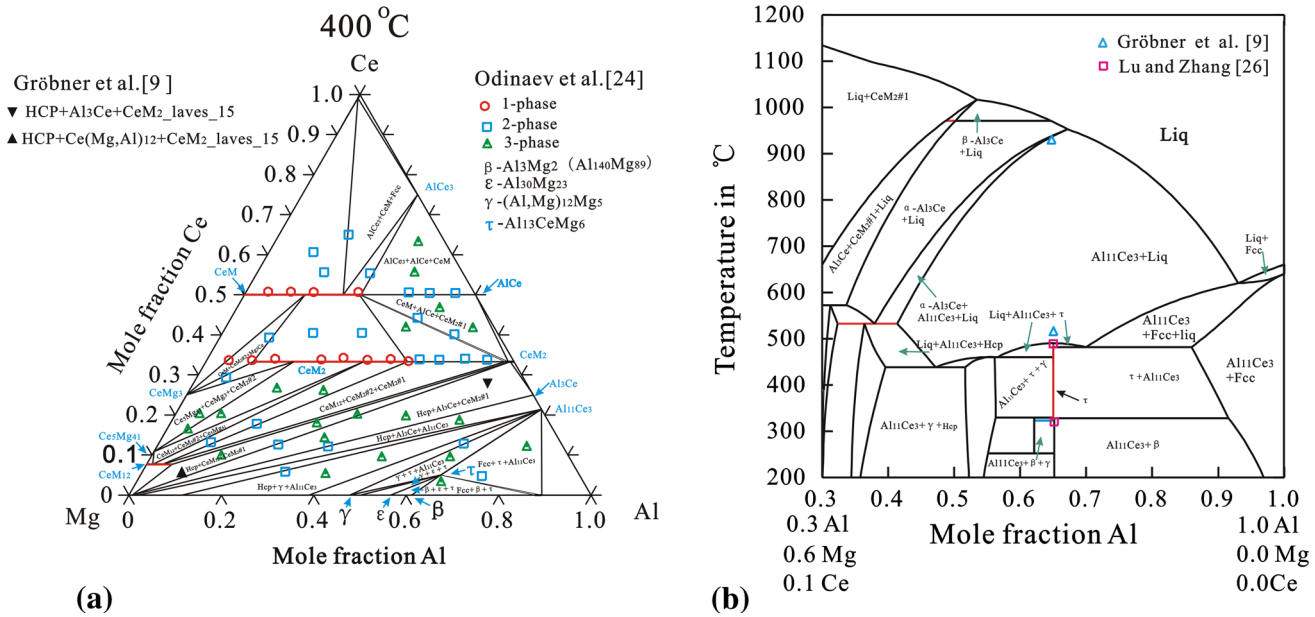

Fig. 3 Calculated (a) isothermal section of the Al-Mg-Ce ternary system at 400 °C and (b) vertical section along Al-Al0.3Mg0.6Ce0.1 (in mole fraction) according to the present assessed thermodynamic descriptions, compared with the corresponding experimental data[9,24,26]

along Al-$Al_{0.3}Mg_{0.6}Ce_{0.1}$ compared with experimental data.[9,26] It can be easily observed that the ternary compound $Al_{13}CeMg_6$ melts at 492.7 °C and decomposes at 327.9 °C. The presently calculated results agree well with the experimental data, but conflict to the assessment results by Gröbner et al.[9] In the work of Gröbner et al.[9] they claimed that the $Al_{13}CeMg_6$ phase melted incongruently at 400 °C and retained at temperature lower than 320 °C, which is not consistent with the recently experimental results by Lu and Zhang.[26]

5.2 Thermodynamic Descriptions for Al-Rich Al-Si-Mg-Ce Quaternary System and Experimental Validation

Considering that there have been no any reports on quaternary compound and phase equilibira in Al-rich Al-Si-Mg-Ce quaternary system in the literature, the thermodynamic database of the Al-rich Al-Si-Mg-Ce quaternary system can be easily established by directly combining the four boundary ternaries adopted/assessed in the present work. To justify the reliability of the established

thermodynamic database, we intend to fully compare the model-predicted microstructure information after solidification and phase transition temperatures in one key model alloy due to the presently established thermodynamic database of the Al-Si-Mg-Ce quaternary system with the experimental data. To do this, the Gulliver-Scheil solidification simulation of the Al-7Si-0.6Mg-0.4Ce alloy was performed, and then comprehensively compared with the experimental data. In the Gulliver-Scheil solidification simulations, diffusion in liquid phase is assumed to be fast enough to achieve the equilibrium immediately, while no diffusion in solid phases is assumed. Such assumptions are acceptable for describing the casting process in, i.e., Al alloys, because the cooling rate is usually large and no fast diffusion species exist in Al alloys.

Figure 4(a) displays the model-predicted solidification curve of the Al-7Si-0.6Mg-0.4Ce alloy under the Scheil condition. As shown on the curve, there are four transitions, i.e., the formation of primary (Al), the binary eutectic reaction Liquid → (Al) + (Si), the ternary eutectic reaction Liquid → (Al) + (Si) + $AlCeSi_2$, and the quaternary eutectic reaction Liquid → (Al) +(Si) + $AlCeSi_2$ + Mg_2Si occurring at 613.8, 571.8, 568.7, and 558.2 °C, respectively. Figure 4(b) displays the heating and cooling DSC curves performed on the Al-7Si-0.6Mg-0.4Ce sample at the heating/cooling rate of 10 °C/min. Three endothermic peaks (i.e., Peaks 1a, 2a, and 3a) are observed in the heating curve, which exactly corresponded to the formation of primary (Al), the binary eutectic reaction Liquid → (Al) + (Si), and the ternary eutectic reaction Liquid → (Al) + (Si) + $AlCeSi_2$. However, no noticeable peak is observed on the heating curve for the quaternary reaction Liquid → (Al) + (Si) + $AlCeSi_2$ + Mg_2Si. That may be attributed to its overlap with the peak for ternary eutectic reaction over the narrow temperature interval at this relatively large heating rate of 10 °C/min.

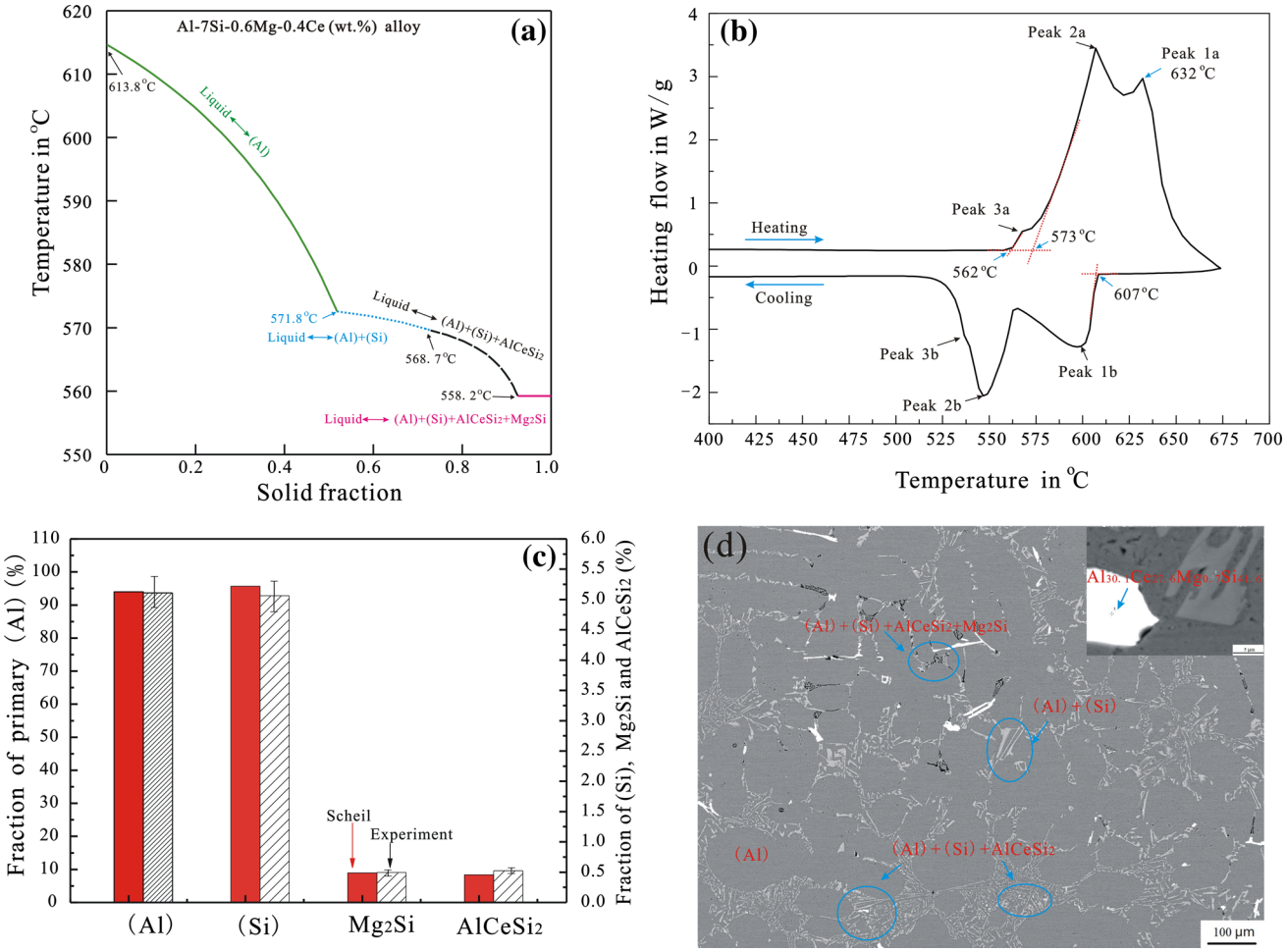

Fig. 4 (a) Model-predicted solidification path of the model alloy (Al-7Si-0.6Mg-0.4Ce) according to the presently established thermodynamic database of the quaternary Al-Si-Mg-Ce system under the Scheil-Gulliver conditions; (b) heating and cooling DSC curves of the mode alloy at a heating/cooling rate of 10 °C/min; (c) model-predicted volume fractions of the primary (Al) and constituent solid phases in eutectic structure of as-cast model alloy, compared with the experimental data; (d) back-scattered electron (BSE) image of the as-cast model alloy

On the cooling curve, only two exothermic peaks (Peaks 1b and 2b) can be clearly observed. The peak corresponding to ternary eutectic reaction (Peak 3b) is very weak in the vicinity of the peak for binary eutectic reaction (Peak 2b). This is due to the overlap of the transition peaks of binary, ternary, and even quaternary eutectic formation over this narrow temperature interval during solidification. For a detail comparison, the calculated phase transition temperatures together with DSC signals are indicated. The calculated results from the Scheil simulation for the binary (571.8 °C) and ternary eutectic reactions (568.7 °C) agree well with the corresponding temperatures of Peaks 2a (573) and 3a (562 °C) during heating. The model-predicted transition temperature for the primary (Al) is 613.8 °C, which is exactly located between Peak 1b (607 °C) during cooling and Peak 1a (632 °C) during heating. The slight deviation from Peak 1b is because the undercooling for the nucleation of primary (Al) is not considered in the Scheil solidification simulation, but the deviation from Peak 1a is because Peak 1a significantly overlaps with the adjacent peak on the heating curve and therefore it is difficult to derive an accurate reaction temperature for the primary (Al) phase.

To further validate the reliability of the established thermodynamic database of the Al-Si-Mg-Ce system, the solidification sequence of the alloy Al-7Si-0.6Mg-0.4Ce was analyzed based on a comparison between the Scheil solidification simulated results and the solidified microstructures. According to Fig. 4(a), the solidification sequence of the alloy is: Liquid → (Al), Liquid → (Al) + (Si), Liquid → (Al) + (Si) + $AlCeSi_2$, and Liquid → (Al) + (Si) + $AlCeSi_2$ + Mg_2Si. Thus, it can be predicted that (Al), (Si), $AlCeSi_2$, and Mg_2Si phases are involved in the final microstructure of the model alloy in the as-cast state, and the primary (Al), binary eutectic (Al) + (Si), ternary eutectic (Al) + (Si) + $AlCeSi_2$, and quaternary eutectic (Al) + (Si) + $AlCeSi_2$ + Mg_2Si constitute the as-cast microstructure. Additionally, the Scheil simulations presented in Fig. 4(a) allow quantitative prediction of the fractions for each constituent solid phase/structure in the as-cast microstructure.[4] For example, the predicted fractions for the solidified (Al), (Si), $AlCeSi_2$ and Mg_2Si phases in the Al-7Si-0.6Mg-0.4Ce alloy are 93.844, 5.22, 0.45, and 0.49 vol.%, respectively, as displayed in Fig. 4(c).

Figure 4(d) displays the BSE image of the as-cast Al-7Si-0.6Mg-0.4Ce alloy. Based on the EPMA composition measurement together with the above Scheil simulations, all the phases involved in the as-cast microstructures of alloy can be characterized. The bright phase present in the microstructure was determined to be $Al_{30.1}Ce_{27.6}Mg_{0.7}Si_{41.6}$ (in at.%), which exactly corresponds to the $AlCeSi_2$ phase though very small solubility of Mg is observed in experiment. In the Fig. 4(d), along the boundary of the primary (Al) phase, a few (Al) + (Si) lamellar eutectic structures that originate from the binary eutectic reaction Liquid → (Al) + (Si) can be observed. Additionally, some fine structures consisting of (Al) + (Si) + $AlCeSi_2$ are observed near the primary (Al), indicating the occurrence of the ternary eutectic transition Liquid → (Al) + (Si) + $AlCeSi_2$. In addition, skeleton-like Mg_2Si phase is also present in the quaternary eutectic structure. Therefore, the solidification sequence, phases and structures involved in the alloy as observed by the experimental BSE images are in excellent agreement with the Scheil prediction based on the presently established thermodynamic database. Additionally, the volume fractions of each constituent solid phase in the as-cast microstructure of the alloy Al-7Si-0.6Mg-0.4Ce were experimentally measured and compared with the Gulliver-Scheil simulated result, as demonstrated in Fig. 4(c). The results show that the experimental data can be accurately reproduced by the calculated results within the estimated experimental errors. It indicated that the presently established thermodynamic database for the Al-Si-Mg-Ce quaternary system in the Al-rich region is reliable. Moreover, based on the present thermodynamic data of Al-Si-Mg-Ce system together with their atomic mobility in liquid and fcc phases,[39] different solidification processes of Al-Si-Mg-Ce multi-component cast alloy have been accurately predicted in our previous work,[39] which further validates the reliability of the thermodynamic database of the Al-Si-Mg-Ce quaternary system in this work.

6 Conclusions

- Based on all the experimental phase equilibria available in the literature, the thermodynamic description of ternary Al-Mg-Ce system was re-assessed via the CALPHAD technique.
- Based on the unified thermodynamic descriptions for all the boundary binaries and adopted/assessed thermodynamic descriptions for boundary ternaries, a self-consistent thermodynamic database of Al-rich Al-Si-Mg-Ce system in the Al-rich region was established via direct extrapolation.
- The reliability of the established thermodynamic database was further validated by comparing the Gulliver-Scheil simulation of a quaternary Al-7Si-0.6Mg-0.4Ce alloy with its experimental phase transition temperatures and microstructure in as-cast alloy. Good agreement between the thermodynamic calculation and experimental results indicates that the present thermodynamic database for the Al-Si-Mg-Ce quaternary system in the Al-rich region is reliable.

Acknowledgments The financial support from the National Natural Science Foundation of China (Grant No. 51474239) and the National Key Research and Development Program of China (Grant No. 2016YFB0301101) is acknowledged. Xi Li thanks Prof. Bo Sundman from INSTN, CEA Saclay, France for his kind help and suggestion on thermodynamic modeling. Lijun Zhang acknowledges financial support from the project supported by State Key Laboratory of Powder Metallurgy Foundation, Central South University, Changsha, China.

References

1. J.G. Kaufman, E.L. Rooy. Aluminum Alloy Castings Properties, Processes, and Applications, ASM International, 2004, p 13–29.
2. A. Hekmat-Ardakan and F. Ajersch, Thermodynamic Evaluation of Hypereutectic Al-Si (A390) Alloy with Addition of Mg, *Acta Mater.*, 2010, **58**(9), p 3422-3428
3. M. Yildirim and D. Özyürek, The Effects of Mg Amount on the Microstructure and Mechanical Properties of Al-Si-Mg Alloys, *Mater. Des.*, 2013, **51**(10), p 767-774
4. Z. Lu and L.J. Zhang, Thermodynamic Description of the Quaternary Al-Si-Mg-Sc System and Its Application to the Design of Novel Sc-Additional A356 Alloys, *Mater. Des.*, 2017, **116**(15), p 427-437
5. A.S. Anasyida, A.R. Daud, and M.J. Ghazali, Dry Sliding Wear Behaviour of Al-12Si-4Mg Alloy with Cerium Addition, *Mater. Des.*, 2010, **31**(1), p 365-374
6. A.M. Nabawy, A.M. Samuel, S.A. Alkahtani, K.A. Abuhasel, and F.H. Samuel, Role of Cerium, Lanthanum, and Strontium Additions in an Al-Si-Mg (A356) Alloy, *Int. J. Mater. Res.*, 2016, **107**(5), p 1-13
7. Y. Tang, Y. Du, L.J. Zhang, X.M. Yuan, and G. Kaptay, Thermodynamic Description of the Al-Mg-Si System Using a New Formulation for the Temperature Dependence of the Excess Gibbs Energy, *Thermochim. Acta*, 2012, **527**(10), p 131-142
8. J. Gröbner, D. Mirkovic, and R. Schmid-Fetzer, Termodynamic Aspects of the Constitution, Grain Refining, and Solidification Enthalpies of Al-Ce-Si Alloys, *Metall. Mater. Trans. A*, 2004, **35**(11), p 3349-3362
9. J. Gröbner, D. Kevorkov, and R. Schmid-Fetzer, Thermodynamic Modeling of Al-Ce-Mg Phase Equilibria Coupled with Key Experiments, *Intermetallics*, 2002, **10**(5), p 415-422
10. L. Jin, D. Kevorkov, M. Medraj, and P. Chartrand, Al-Mg-RE (RE = La, Ce, Pr, Nd, Sm) Systems: Thermodynamic Evaluations and Optimizations Coupled with Key Experiments and Miedema's Model Estimations, *J. Chem. Thermodynamics*, 2013, **58**(3), p 166-195
11. G. Cacciamani and R. Ferro, Thermodynamic Modeling of Some Aluminium-Rare Earth Binary Systems: Al-La, Al-Ce and Al-Nd, *Calphad*, 2001, **25**(4), p 583-597
12. M.C. Gao, N. Ünlü, G.J. Shiflet, M. Mihalkovic, and M. Widom, Reassessment of Al-Ce and Al-Nd Binary Systems Supported by Critical Experiments and First-Principles Energy Calculations, *Metall. Mater. Trans. A*, 2005, **36**(12), p 3269-3279
13. L.L. Jin, Y.-B. Kang, P. Chartrand, and C.D. Fuerst, Thermodynamic Evaluation and Optimization of Al-La, Al-Ce, Al-Pr, Al-Nd and Al-Sm Systems Using the Modified Quasichemical Model for Liquids, *Calphad*, 2011, **35**(1), p 30-41
14. G. Cacciamani, A. Saccone, R. Ferro, I. Ansara, A.T. Dinsdale, M.H. Rand (Eds.). COST 507: Thermochemical Database for Light Metal Alloys, vol. 2, European Commission, 1998, pp. 137–140.
15. H. Zhang, Y. Wang, S.L. Shang, L.Q. Chen, and Z.K. Liu, Thermodynamic Modeling of Mg-Ca-Ce System by Combining First-Principles and CALPHAD Method, *J. Alloys Compd.*, 2008, **463**(2), p 294-301
16. X. Li, Phase Equilibrium, Thermodynamic Modeling and Application of the A1-Mg-Ce, A1-Mg-Zr and A1-Mg-Sc-Zn Systems. Master thesis, Central South University, Changsha, China, 2014, pp. 11–18.
17. L.N. Altunina, E.I. Gladyshevsky, O.S. Zarechnyuk, and I.F. Kolobnev, Physico-Chemical Properties of Al-Si-Ce with 0 to 73 wt.% Ce, *Zh. Neorg. Khim.*, 1963, **8**(2), p 870-873
18. A. Raman and H. Steinfink, Crystal Chemistry of AB_2 Structures. I. Investigations on AB_2 Sections in the Ternary Systems Rare Earth-Aluminum-Silicon,-Germanium, and-Tin, *Inorg. Chem.*, 1967, **6**(10), p 1789-1795
19. A.A. Murav'eva. Phase Equilibria and Crystal Structure of Compounds in Ternary Systems of Aluminium and Silicon (Germanium) with Rare Earth Metals, Autorreferat Dis. Kand. Khim. Abstract of Thesis, Nauk. Lvov, 1972, pp. 1–18.
20. H. Flandorfer, D. Kaczorowski, J. Gröbner, P. Rogl, R. Wouters, C. Godart, and A. Kostikas, The Systems Ce-Al-(Si, Ge): Phase Equilibria and Physical Properties, *J. Solid State Chem.*, 1998, **137**(2), p 191-205
21. H. Flandorfer and P. Rogl, The Crystal Structure of Two Novel Compounds: $CeAlSi_2$ and $Ce_3Al_4\ Si_6$, *J. Solid State Chem.*, 1996, **127**(2), p 308-314
22. O.S. Zarechnyuk and P.I. Kripyakevich, X-ray Structural Investigation of the Ce–Mg–Al System in the Range 0–33.3 at.% Ce, *Russ. Metall.*, 1967, **4**, p 101-103
23. Z. Cui and R. Wu, Phase Diagram and Properties of Ternary Al-Mg-Ce Alloys, *Acta Metall. Sin.*, 1984, **20**(6), p 323-331
24. K.O. Odinaev, I.N. Ganiev, V.V. Kinzybalo, and H.R. Kurbanov, Phase Equilibria in the Al–Mg–Y and Al–Mg–Ce Systems at 673 K, *Izvvyssich ucebnych zavedenij, Cvetnaja metallurgija*, 1989, **2**, p 75-77
25. K.O. Odinaev, I.N. Ganiev, and A.Z. Ikromov, Pseudobinary Sections and Liquidus Surface of the Al–Mg–$CeAl_2$ System, *Russ. Metall.*, 1996, **3**, p 122-125
26. Z. Lu and L.J. Zhang, Thermal Stability and Crystal Structure of High-Temperature Compound $Al_{13}CeMg_6$, *Intermetallics*, 2017, **88**(9), p 73-76
27. C. Zheng, Y. Wu, J. Qian, and Y. Ye, Liquidus and Intermetallic Compound in Al-Rich Region of Al–Mg–Ce System, *Acta Metall. Sin.*, 1986, **22**(2), p 63-67
28. O. Redlich and A.T. Kister, Algebraic Representation of Thermodynamic Properties and the Classification of Solutions, *J. Ind. Eng. Chem.*, 1948, **40**(2), p 84-88
29. D. Hao, B. Hu, K. Zhang, L.J. Zhang, and Y. Du, The Quaternary Al–Fe–Ni–Si Phase Equilibria in Al-Rich Corner: Experimental Measurement and Thermodynamic Modelling, *J. Mater. Sci.*, 2014, **49**(3), p 1157-1169
30. A.T. Dinsdale, SGTE Data for Pure Elements, *Calphad*, 1991, **15**(4), p 317-425
31. L.J. Zhang, J. Wang, Y. Du, R.X. Hu, P. Nash, X.G. Lu, and C. Jiang, Thermodynamic Properties of the Al-Fe-Ni System Acquired Via a Hybrid Approach Combining Calorimetry, First-Principles and CALPHAD, *Acta Mater.*, 2009, **57**(18), p 5324-5341
32. B. Sundman and J. Ågren, A Regular Solution Model for Phases with Several Components and Sublattices, Suitable for Computer Applications, *J. Phys. Chem. Solids*, 1981, **42**(4), p 297-301
33. W.D. Zhang, Y. Liu, J. Yang, J.Z. Dang, H. Xu, and Z.M. Du, Effects of Sc Content on the Microstructure of As-Cast Al-7 wt.%Si Alloys, *Mater. Charact.*, 2012, **66**(4), p 104-110
34. B. Sundman, B. Jansson, and J.O. Andersson, The Thermo-Calc Databank System, *Calphad*, 1985, **9**(2), p 153-190

35. A. Saccone, D. Macciò, S. Delfino, F.H. Hayes, and R. Ferro, Mg–Ce Alloys: Experimental Investigation by Smith Thermal Analysis, *J. Therm. Anal. Calorim.*, 2001, **66**(1), p 47-57
36. R. Vogel and T. Heumann, Determination of Ce-Mg and La-Mg Systems, *Z. Metallkd.*, 1947, **38**, p 1-8
37. D.H. Wood and E.M. Cramer, Phase Relations in the Magnesium-Rich Portion of the Cerium-Magnesium System, *J. Less-Common Met.*, 1965, **9**(5), p 321-337
38. J.L. Haughton and T.H. Schofield, Alloys of Magnesium. PartV: The Constitution of the Magnesium Rich Alloys of Magnesium and Cerium, *J. Inst. Met.*, 1937, **60**, p 339-344
39. Z. Lu, Y. Tang, and L.J. Zhang, Atomic Mobility in Liquid and Fcc Al-Si-Mg-RE (RE = Ce, Sc) Alloys and Its Application to the Simulation of Solidification Processes in RE-Containing A357 Alloys, *Int. J. Mater. Res.*, 2017, **108**(6), p 465-476